National Weather Service
Office of Meteorology

Technical Procedures Bulletin

Subject:

Probability Forecasts of Clear-Air-Turbulence for the Contiguous US

Series No. 430

Science Division Science & Training Core Silver Spring, Md. 20910

FIRST BULLETIN ON THIS SUBJECT

February 2, 1996
W/OM21:MEH

This bulletin, written by Ronald M. Reap of the Techniques Development Laboratory, describes the new NGM-based 6-h probability forecasts of nonconvective clear-air-turbulence (CAT) for the contiguous U.S. that have been produced daily in a non-operational mode for the National Centers for Environmental Prediction's (NCEP's) Aviation Weather Center (AWC) and Hydrometeorological Prediction Center (HPC) since August 16, 1995. The probability equations were developed from forecast fields from the NCEP's Nested Grid Model (NGM) (Hoke et. al. 1989), national lightning location data (Krider et al. 1976), and pilot reports (PIREPS) from the AWC's data archives. This TPB is the first to describe the new forecast products for predicting CAT. The forecasts were designed to provide general objective guidance in the 2-26 h timeframe to forecasters at AWC and HPC. AWC is responsible for issuing operational AIRMETS and SIGMETS which are inflight advisories for use the aviation community.

The new forecasts are valid for the 2-8 h, 8-14 h, 14-20 h, and 20-26 h projections after 0000 and 1200 UTC initial data times. They give the unconditional probability of category 3 (light-to-moderate) and category 5 (moderate-to-severe) or greater CAT occurring in grid blocks that are 48-km on a side. Separate forecasts are produced for the high-band (> 15,000 ft AGL) and low-band (<15,000 ft AGL) regions.

Joseph R. Bocchieri
Chief, Science and Training Core

PROBABILITY FORECASTS OF CLEAR-AIR-TURBULENCE FOR THE CONTIGUOUS U.S.

by Ronald M. Reap, Techniques Development Laboratory

1. INTRODUCTION

This bulletin describes the new NGM-based 6-h probability forecasts of nonconvective clear-air-turbulence (CAT) for the contiguous U.S. that have been produced daily in a non-operational mode for the National Centers for Environmental Prediction's (NCEP's) Aviation Weather Center (AWC) and Hydrometeorological Prediction Center (HPC) since August 16, 1995. The probability equations were developed from forecast fields from the NCEP's Nested Grid Model (NGM) (Hoke et. al. 1989), national lightning location data (Krider et al. 1976), and pilot reports (PIREPS) from the AWC's data archives. The probability forecasts are valid for the 2-8 h, 8-14 h, 14-20 h, and 20-26 h projections after 0000 UTC and 1200 UTC initial data times. The forecast equations give the unconditional probability of category 3 (light-to-moderate) or greater and category 5 (moderate-to-severe) or greater CAT occurring in grid blocks that are approximately 48 km on a side covering the contiguous United States. The new probability forecasts were designed to provide general objective guidance in the 2-26 h timeframe to forecasters at the aviation operations branch of AWC located in Kansas City, MO. AWC is responsible for issuing operational AIRMETS and SIGMETS which are inflight advisories for use by the aviation community.

2. DEVELOPMENT

a. Method

The CAT forecast equations were derived by applying screening regression techniques and the Model Output Statistics (MOS) approach (Glahn and Lowry 1972) to relate the PIREP predictand data to large-scale meteorological predictors obtained from the NGM. National lightning location data were used to eliminate CAT reports arising from localized thunderstorm activity. As a result, the forecast equations predict the probability of occurrence of nonconvective CAT. Separate equations were developed for the eastern and western U.S. to accommodate the unique meteorological conditions related to CAT over the western mountains. Equations were developed for the high-band (> 15,000 ft above ground level (AGL)) and low-band (< 15,000 ft AGL) regions. Strictly speaking, turbulence below about 5,000 ft AGL is generally mechanical in nature and not referred to as CAT. All reports below 15,000 ft AGL were, however, used in the MOS development effort in order to provide as broad a response as possible by the forecast equations to varying atmospheric conditions, especially over the western mountains. Separate forecast equations were also developed for the warm season (March 16 - September 30) and cool season (October 1 - March 15) periods.

b. Predictand Sample

PIREP data were obtained from AWC for the three-year period from 1988-90. Like many observed datasets, PIREPS suffer from specific limitations. They are intermittent in both space and time and are relatively scarce at night when few aircraft are aloft. Reports of CAT are subjective in nature and, therefore, uncalibrated since they depend upon the pilot's perception of the degree of turbulence, which

in turn depends upon the weight, speed, and aerodynamic characteristics of the aircraft being flown. Despite these limitations, the present developmental effort was successful in using the PIREPS to identify significant areas of CAT that were related to major features in the large-scale flow.

During initial processing, the reported CAT events, whose positions are given by latitude and longitude in the PIREPS, were related to an 89x113 grid covering the contiguous United States (Fig. 1). The maximum value of CAT observed during the hour was tabulated and stored for each 48-km grid block in the 89x113 array, i.e., if multiple CAT events were reported for an individual 48-km grid block, only the maximum value was saved. The archived turbulence intensity for each grid block was indicated by the category values that were originally used to encode the PIREPS, i.e.,

1 = Smooth to light
2 = Light
3 = Light to moderate
4 = Moderate
5 = Moderate to severe
6 = Severe
7 = Severe to extreme
8 = Extreme

In processing the PIREP data, a CAT event was considered to have occurred when turbulence intensities of 3 or greater were reported. Turbulence intensities of 3 and 4 were, however, accepted as valid CAT events only if they were reported by aircraft of 10,000 lbs or greater, i.e., generally twin-engine aircraft and larger. Weight data in the processing program were obtained from tables of common aircraft types and specifications, including both civilian and military aircraft (Arkell 1992). Aircraft weights were extracted from the tables and compared to the CAT intensity for each report analyzed during the hourly tabulations. Reports from aircraft less than 10,000 lbs are considered to be biased since small aircraft are more easily affected by turbulence and tend to report higher intensities than large commercial or military aircraft under similar flight conditions. This bias is illustrated in Fig. 2, which shows the distribution of CAT intensity levels during 1990 for the high-band and low-band regions. All categories in the low band above category 2 show a higher percentage of reported CAT events relative to the high band, reflecting the tendency for smaller aircraft to report higher intensities. During the processing, turbulence intensities of 5 or greater were, however, accepted as valid CAT events regardless of aircraft weight.

For a CAT event with multiple latitudes and longitudes, i.e., a line segment, or dogleg in the case of three sets of latitudes and longitudes, the event was assigned to all 48-km grid blocks through which the line segment(s) passed. Line or dogleg segments over 300 mi (480 km) were, however, not used due to the likelihood of reporting errors. Aviation forecasters at AWC have observed through experience that segments over 300 mi are sometimes unreliable. In general, most line segments are reported by general aviation pilots in the low-band region below 15,000 ft. Above 15,000 ft, airline and military pilots usually give point reports of turbulence.

As previously noted, national lightning location data were used to eliminate any CAT events associated with thunderstorm activity. In effect, a value of zero was stored for 48-km grid blocks where one or more cloud-to-ground flashes were reported during the hour. Grid blocks immediately adjacent to a thunderstorm area were also zeroed to reduce the possibility of contaminating the sample with convective CAT events.

c. Predictor Sample

CAT is a mesoscale phenomenon that is not resolvable at the grid spacing of the NGM forecast model. The NGM predictors offered to the screening regression procedure are, therefore, designed to identify large-scale synoptic flow patterns that are related to the occurrence of CAT. This approach has been successfully employed in previous MOS developmental efforts to predict other mesoscale weather elements, e.g., thunderstorms and severe local storms (Reap and Foster 1979). The predictor sample included a set of basic and derived predictors from the NGM. Table 1 lists the NGM predictors that were offered to the screening regression procedure. Since the generation of CAT is closely related to atmospheric stability, various measures of temperature lapse rate, the Total Totals index (Miller 1972), and K index (George 1960) were included in Table 1. Also included in Table 1 were several predictors known to be related to CAT, e.g., shearing and stretching deformation, total deformation, and the TI1 and TI2 indices developed by Mancuso and Endlich (1966) and operationally applied by Ellrod and Knapp (1992). Deformation is a quantifiable kinematic predictor that acts to strengthen upper-level frontal zones by increasing the horizontal temperature gradients, thereby increasing the likelihood of CAT occurrence.

The deformation predictors are given by:

$$\text{Shearing deformation} = DSH = \partial v/\partial x + \partial u/\partial y$$

$$\text{Stretching deformation} = DST = \partial u/\partial x - \partial v/\partial y$$

$$\text{Total deformation} = DEF = (DSH^2 + DST^2)^{1/2}$$

where u and v are the horizontal wind components.

TI1 and TI2 are computed over specified layers and are given by:

$$TI1 = VWS \times DEF$$

$$TI2 = VWS \times (DEF + CVG)$$

where VWS is the vertical wind shear and CVG is the horizontal mass convergence computed for the specified layer as given by:

$$CVG = -(\partial u/\partial x + \partial v/\partial y)$$

The TI1 values are in units of 10^{-7} sec^{-2} and range in value from 0 to 15 units. Figure 3 shows the relationship derived from the 1988-90 developmental cool-season sample between the TI1 index and observed CAT frequencies (x 10) of 3 or greater for the 20-26 h projection after 0000 UTC. The effectiveness of the TI1 predictor in predicting significant CAT is indicated in Fig. 3 by the highly linear relationship between TI1 and CAT. Strong vertical wind shear can also result in the generation of turbulent eddies and ensuing CAT. When vertical wind shear is combined with deformation and horizontal convergence in the TI1 and TI2 indices, important predictors are created that simulate the nonlinear interactions among the three predictors.

Many of the predictors shown in Table 1 are interactive, or combined, predictors (Reap and Foster 1979), including the original formulations of TI1 and TI2 developed by Mancuso and Endlich (1966). Other interactive predictors in Table 1 include the vertical velocity, deformation, and vertical wind shear combined with various synoptic fields known to be related to CAT, i.e., temperature lapse rate, horizontal temperature gradient, wind speed, temperature advection, and horizontal convergence. The function of the interactive predictors is partially to account for the particular, diverse, and probably nonlinear combinations of conditions that can lead to the occurrence of the predictand event. The selected variables are expected to interact with or complement one another in predicting the event. The total deformation multiplied by the wind speed (Table 1), for example, simulates the nonlinear interaction between two individual predictors representing synoptic fields that are significant in the formation of CAT. This predictor was selected as the lead predictor in several of the probability equations. It is interesting to note that previous studies (Dutton 1980; Mancuso and Endlich 1966) found wind speed to be poorly related to CAT. In the present study, however, wind speed was found to be important when interactively combined with other synoptic variables, such as total deformation. Previous studies have also shown no clear consensus as to the relative order of importance of many of the predictors in Table 1 to the occurrence of CAT. In the present study, we are dealing with a very large developmental data sample; therefore, the MOS screening regression procedure should generate stable and reliable statistical relationships between the predictors and the occurrence of CAT.

d. Unconditional CAT Probability Equations

Linear screening regression and the MOS approach were used to develop forecast equations that give the unconditional probability of CAT for both the warm (March 15 - September 30) and cool seasons (October 1 - March 14). Initially, 12-term forecast equations were developed for each region in Fig. 1 for the four valid periods (2-8, 8-14, 14-20, and 20-26 h) following the 0000 and 1200 UTC initial data times. To enhance forecast consistency, a representative list of 12 predictors was assembled based on the individual predictor lists for the separate runs for each region. The screening regression procedure was repeated by forcing selection of these 12 predictors, thereby, helping to ensure forecast consistency from one valid period to the next. The analysis of CAT reports and forecast model fields was limited to the grid blocks within the contiguous U.S. landmass (Fig. 1); no over-water grid blocks were used in the regression procedure.

The resulting forecasts represent the unconditional probability of CAT intensities of 3 or greater and 5 or greater occurring in 48-km grid blocks during each of the 6-h valid periods. Forecasts are produced for the 2-8 h, 8-14 h, 14-20 h, and 20-26 h periods following 0000 and 1200 UTC. The forecasts for category 3 are available as guidance to forecasters at AWC for issuing operational AIRMETS while the category 5 forecasts are available as guidance in issuing SIGMETS. Separate forecast equations were developed for the eastern and western U.S.; the two regions are shown in Fig. 1. Each equation was developed from a generalized dataset created by combining data from all grid blocks in each region. The total sample size for the East was about 1.2 million cases (2949 overland grid blocks times 409 sample days) for the 1988-90 cool seasons. For the West, the cool-season sample size was about 0.7 million cases (1728 blocks times 409 days). For the warm season, the sample size was 1.7 million cases for the East and 1.1 million cases for the West. These represent very large samples (588 days) which should result in stable and reliable forecast equations.

CAT frequency, or the fraction of 48-km grid blocks with CAT intensities of 3 or greater, was generally less than 1.0% for the individual 6-h forecast projections during the warm and cool season developmental samples. CAT is a rare event relative to the total number of forecasts generated for the small 48-km grid blocks shown in Fig. 1. In Fig. 2, about 70% (40%) of the high-band (low-band) reports are intensity levels of 2 or less, which are considered non-events in the screening regression analysis definition of significant CAT. Predictand frequency and the resulting range of forecast probabilities are also directly related to grid

block size. Small grid blocks result in lower frequencies since a smaller geographical area is "verified" by a given occurrence of CAT.

Table 2 shows the 12 predictors in the cool-season CAT forecast equations for the eastern and western United States for the high-band region above 15,000 ft for the four 6-h projections after 0000 and 1200 UTC. Predictors are listed in the order of importance in terms of their contribution to the cumulative reduction of variance. It is interesting to note that 50% of the predictors in Table 2 are interactive (combined) predictors. The leading predictor for both East and West in Table 2 is an interactive predictor giving the product of the total deformation and wind speed at 300 mb. The 700-mb wind speed and 500-850 mb temperature lapse rate are important predictors over the western U.S., where mechanically-induced turbulent eddies can form in the lee of the mountains under conditions of strong flow normal to the mountain ridges and favorable temperature lapse rates. The 500-mb u and 300-mb v wind components selected for the eastern U.S. suggest that wind velocity is important when selected in combination with other predictors by the screening regression analysis. In previous studies (Mancuso and Endlich 1966; Dutton 1980), wind speed, by itself, did not prove to be a very good predictor of CAT. In the present study, however, wind speed in linear or interactive combination with other predictors appears to be an important predictor of CAT. Sine day-of-year provides a climatic contribution to the probability forecasts. The selection of relative humidity and the K stability index reflect the influence of moisture and stability in conjunction with the selected kinematic predictors in Table 2.

Table 3 is similar to Table 2, except that it shows the 12 predictors for the low-band below 15,000 ft. As expected, low-level predictors were primarily selected in the low-band equations. In a general physical sense, the highest probabilities in the eastern U.S. are forecast in regions characterized by deformation combined with vertical wind shear, low pressure at the surface, high wind speed at 700 mb and cold-air temperature advection at 850 mb. Wind speed and wind components at 700 mb are even more important in the West where low-band turbulence is often related to flow normal to the mountain ridges. Other important predictors for the West include deformation, vertical wind shear, and 850-mb temperature advection. Cosine day-of-the-year again reflects a climatic contribution to the probability forecasts.

3. Verification

As previously noted, CAT frequencies were less than 1% for the individual 6-h forecast projections resulting in a probability range of about 0 to 4% for the MOS forecasts. Probabilities for category 3 or greater CAT were, therefore, scaled by a multiplicative factor of 20 for both low and high bands. Probabilities for category 5 or greater CAT were scaled by multiplicative factors of 40 for the low band and 80 for the high band. Hereafter, use of the term "probability" refers to the scaled probability values. The reliability or bias of the operational CAT equations was evaluated by computing frequencies for six CAT probability categories, where the scaled values range from 0-10% to 50-60%. To compute the frequency for each of the scaled forecast categories, the total number of observed grid blocks with CAT intensities of 3 or greater (5 or greater) in each forecast category was divided by the total number of daily forecasts or grid blocks in that category. For example, the reliability of the cool season probability forecasts for category 3 or greater CAT for the 14-20 h projection for the high-band region is shown in Fig. 4. The data points are located at the average scaled forecast probability for each of the six categories. The number of forecasts (plotted in thousands) is also shown next to each data point. The unlabeled diagonal line represents perfect forecast reliability or zero bias. Figure 4 indicates that the CAT probability forecasts were reliable for the 1988 dependent data sample with only a slight tendency to overforecast in the middle ranges. Similar verification statistics were obtained for the remaining forecast projections in the dependent data sample. Based on our experience with previous MOS developmental forecast equations, no significant degradation is anticipated in the verification statistics for independent data samples.

To further examine the usefulness of the probability forecasts to the operational forecaster, we produced categorical or yes/no forecasts of CAT based on the grid block probabilities. The expected accuracy of such forecasts as a function of various scaled probability threshold values is indicated in Fig. 5 for category 3 or greater CAT in the high-band. The threshold values are, in effect, scaled probability values that could be selected by the forecaster to delineate the regions where CAT is expected to occur. Fig. 5 contains several scores suggested by Donaldson et al. (1975). Table 4 shows the contingency table used in computing the scores. The scores computed are the probability of detection (POD), given by x/(x+y), the false alarm ratio (FAR), given by z/(x+z), and the critical success index (CSI), given by x/(x+y+z). Due to the relative rarity of CAT, most grid blocks contain no CAT reports; hence, the FAR in Fig. 5 is uniformly high resulting in correspondingly low values for the CSI. The POD, therefore, is the primary score to be considered in this discussion. The probability forecast of category 3 or greater CAT in Fig. 6 can be used to illustrate the effect of selecting one of the various probability threshold values based on the POD in Fig. 5. If, for example, a threshold value of 15% is selected from Fig. 5, then the area defined by this probability isoline would be expected, on average, to contain about 75% of the observed CAT events, as shown by the POD in Fig. 5. Selection of an appropriate threshold value by the local forecaster is ultimately based on experience gained by using the probability guidance over an extended period of time.

4. Forecast Considerations

Predictand frequency and the resulting range of forecast probabilities are directly related to grid block size. Small grid blocks will automatically result in lower predictand frequencies, a limited range of forecast probabilities, and higher scores for the FAR and CSI. These trends occur since a smaller geographical area (and, consequently, a lower percentage of grid blocks) is "verified" by a given CAT event. As a result, the NGM-based CAT probability forecasts range between 0 and 4%, considerably less than previous MOS probability forecasts, e.g., Reap and Foster (1979). The lower probability forecasts from the NGM-based CAT probability equations are, in effect, a direct result of the relative rarity of CAT and the small 48-km grid blocks used in equation development. To assist the forecaster in ease of pattern recognition, the category 3 or greater and 5 or greater CAT probability forecasts were inflated, i.e., multiplied by factors of 20 and 40, respectively. The MOS forecast for category 3 or greater CAT shown in Fig. 6, for example, corresponds to contours indicating a scaled (actual) probability range of 0% to 35% (0% to 1.75%).

Significant diurnal variations in the magnitude of the probabilities from one 6-h interval to the next were found in the initial test forecasts due to the temporal variability in the reported CAT events. Relatively low frequencies are reported at night, for example, during the 2-8 h interval after 0000 UTC and the 14-20 h interval after 1200 UTC (9 p.m. to 3 a.m.) when relatively few aircraft are aloft. In contrast, the highest CAT frequencies are reported during the day for the 14-20 h interval after 0000 UTC and the 2-8 h interval after 1200 UTC (9 a.m. to 3 p.m.) when aircraft traffic is at a maximum. In effect, the CAT forecasts give the probability of CAT being reported during each of the forecast projections. To compensate for the pronounced diurnal variability, the forecasts for the 9 a.m. to 3 p.m. (maximum reported CAT frequency) and 9 p.m. to 3 a.m. (minimum reported CAT frequency) forecast projections were calibrated to ensure consistency with the magnitudes of the probability forecasts for the remaining forecast projections. The calibration procedure preserves the forecast patterns for the intervals to be adjusted and simply modifies the magnitudes to be consistent with those found in the preceding and following projections.

The operational forecasts are, therefore, not true probabilities since they have been scaled to provide sufficient magnitudes for objective analysis and display and calibrated to ensure consistency in the forecast magnitudes from one projection to the next. These modifications are justified on the basis that the observed frequencies of CAT are not true observed frequencies since they depend directly upon the average number of aircraft aloft during any given projection. The modified forecasts should, therefore, be viewed as indices of CAT occurrence rather than true probabilities. In any case, the areal patterns are of paramount interest to the forecaster. Continued daily use of the scaled and calibrated CAT forecasts

should allow the forecaster to develop a "feel" for the magnitudes and how they relate to the number and severity of observed CAT. In effect, the magnitude of the CAT probability forecast is not nearly as important as the ability to accurately delineate the potential areal extent of turbulent outbreaks. The areas defined by the probability threshold values are available to operational forecasters at AWC for planning purposes and for preparing AIRMETS and SIGMETS. Selection of an appropriate threshold value, based on verification statistics, should result in objectively determined areas of expected CAT similar in size to those on manual products issued by operational forecasters.

The new NGM-based MOS forecasts of CAT should be operationally useful to the forecaster for several reasons. Use of lightning data, for example, to remove convectively-generated CAT gives an improved definition of the CAT predictands which should result in better statistical relationships with the NGM predictors. Use of relatively small (48 km) grid blocks allows the CAT forecast equations to locate and define CAT maxima more accurately, as shown, for example, by the narrow band of probabilities across the eastern states in Fig. 6. The pattern of CAT in Fig. 6 is typical of that associated with jet stream patterns found with upper-level cutoff lows. Finally, the relatively large 3-year sample of predictor and predictand data should result in more stable and accurate forecast equations. As is the case with all MOS forecasts, however, the new NGM-based probability forecasts are highly dependent upon the accuracy of the NGM forecasts used as input. Therefore, the probability guidance may have to be used with caution if the forecaster detects possible errors in the model predictions.

5. Graphics Products

The MOS probability forecasts of CAT are generated twice daily at NCEP. The output files are transmitted as NTRANS CGM metafiles to AWC in Kansas City, Missouri. The files are subsequently unpacked and processed for display on AWC's GEMPAK system using the NTRANS graphical user interface. Within the context of the GEMPAK system, the CAT graphical products can be animated or looped as desired. Combined displays can also be generated with the CAT forecasts and selected meteorological fields, such as the 300-mb chart, 850-mb chart, etc., appearing on the same display. These options can be controlled by the forecaster to achieve maximum utility of the graphical CAT probability displays.

6. References

Arkell, R. E., 1992: Aircraft specifications. A reference for aviation weather forecasting. Nat. Wea. Digest, 17, 18-32.

Donaldson, R. J., Jr., R. M. Dyer, and M. J. Kraus, 1975: An objective evaluator of techniques for predicting severe weather events. Preprints Ninth Conference Severe Local Storms, Norman, Amer. Meteor. Soc., 321-326.

Dutton, M. J. O., 1980: Probability forecasts of clear-air-turbulence based on numerical model output. Meteorol. Mag., 109, 293-310.

Ellrod, G. P., and D. I. Knapp, 1992: An objective clear-air-turbulence forecasting technique: Verification and operational use. Wea. Forecasting, 7, 150-165.

George, J. J., 1960: Weather Forecasting for Aeronautics. *Academic Press*, 673 pp.

Glahn, H. R., and D. A. Lowry, 1972: The use of Model Output Statistics (MOS) in objective weather forecasting. J. Appl. Meteor., 11, 1203-1211.

Hoke, J. E., N. A. Phillips, G. J. Dimego, J. J. Tuccillo, and J. G. Sela, 1989: The regional analysis and forecast system of the National Meteorological Center. Wea. Forecasting, 4, 323-334.

Krider, E. P., R. C. Noggle, and M. A. Uman, 1976: A gated wideband magnetic direction finder for lightning return strokes. J. Appl. Meteor., 15, 301-306.

Mancuso, R. L., and R. M. Endlich, 1966: Clear air turbulence frequency as a function of wind shear and deformation. Mon. Wea. Rev., 94, 581-585.

Miller, R. C., 1972: Notes on analysis and severe storm forecasting procedures of the Air Force Global Weather Central. Air Weather Service Tech. Rep. 200 (Rev.), U.S. Air Force, 102 pp.

Reap, R. M., and D. S. Foster, 1979: Automated 12-36 hour probability forecasts of thunderstorms and severe local storms. J. Appl. Meteor., 18, 1304-1315.

Table 1. Variables from the NGM offered as predictors to the screening regression analysis.

Predictor (level, if applicable)
Temperature (300 mb)
Temperature gradient (300 mb)
Temperature advection (850, 500, 300 mb)
Relative humidity (500, 300 mb)
Mean relative humidity (MRH) (1000-500 mb)
u horizontal wind comp (700, 500, 300 mb)
v horizontal wind comp (700, 500, 300 mb)
Wind speed (700, 500, 300 mb)
Sea-level pressure
Height (1000, 850, 500 mb)
Vorticity advection (500 mb)
MRH times Total Totals stability index
MRH times K stability index
Vertical velocity times relative humidity (700, 500, 300 mb)
TI1 index (850, 700, 500, 300 mb)
TI2 index (850, 700, 500, 300 mb)
Layer TI1 index (950-850, 850-700, 700-500, 500-300 mb)
Layer TI2 index (950-850, 850-700, 700-500, 500-300 mb)
Total deformation (850, 700, 500, 300 mb)
Layer total deformation (950-850, 850-700, 700-500, 500-300 mb)
Layer stretching deformation (950-850, 850-700, 700-500, 500-300 mb)
Layer shearing deformation (950-850, 850-700, 700-500, 500-300 mb)
Total deformation (300 mb) times temperature lapse rate (300-500 mb)
Total deformation times temperature gradient (300 mb)
Total deformation times temperature advection (300 mb)
Total deformation times wind speed (300 mb)
Vertical wind shear (300-500 mb) times temperature lapse rate (300-500 mb)
Vertical wind shear (300-500 mb) times temperature gradient (300 mb)
Vertical wind shear (300-500 mb) times temperature advection (300 mb)
Vertical wind shear (300-500 mb) times wind speed (300 mb)
Vertical wind shear (300-500 mb) times total deformation (300 mb) plus wind speed (300 mb)
Vertical wind shear (300-500 mb) times total deformation (300 mb) plus temperature advection (300 mb)
Vertical wind shear (300-500 mb) times total deformation (300 mb) plus temperature gradient (300 mb)
Total deformation plus horizontal convergence (300 mb)
Wind shear (950-500, 850-300, 850-500, 700-500 mb)
Wind divergence (950 mb)
Vorticity advection (500 mb)
Temperature lapse rate (300-500, 500-700, 500-850, 700-850 mb)
Height of freezing level
Sine day-of-year
Cosine day-of-year

Table 2. NGM predictors in cool season MOS probability equations for category 3 or greater CAT for the high-band region for the 2-8 h, 8-14 h, 14-20 h, and 20-26 h projections following 0000 and 1200 UTC.

Eastern U.S.	Western U.S.
300-mb total deformation times 300-mb wind speed	300-mb total deformation times 300-mb wind speed
850-mb TI2 index	700-mb wind speed
300-mb v wind component	500-850 mb temperature lapse rate
1000-500 mb mean relative humidity times K stability index	300-mb total deformation times 300-500 mb lapse rate
Sine day-of-year	Sine day-of-year
300-500 mb vertical wind shear times 300-mb wind speed	850-mb temperature advection
Freezing level	Freezing level
300-mb total deformation times 300-500 mb lapse rate	500-300 mb shearing deformation
500-mb u wind component	500-mb TI1 index
300-mb vertical wind shear times 300-mb total deformation plus temperature gradient	300-500 mb vertical wind shear times 300-mb total deformation plus 300-500 mb lapse rate
300-mb relative humidity	950-850 mb TI2 index
850-mb total deformation	1000-500 mb mean relative humidity times K stability index

Table 3. NGM predictors in cool season MOS probability equations for category 3 or greater CAT for the low-band region for the 2-8 h, 8-14 h, 14-20 h, and 20-26 h projections following 0000 and 1200 UTC.

Eastern U.S.	Western U.S.
850-mb TI1 index	700-mb wind speed
1000-mb height	950-850 mb TI1 index
700-mb wind speed	Freezing level
500-mb v wind component	850-mb temperature advection
850-mb temperature advection	500-mb TI2 index
Cosine day-of-year	700-mb u wind component
850-mb TI2 index	700-mb v wind component
700-500 mb TI2 index	Sine day-of-year
700-500 mb shearing deformation	850-mb TI2 index
850-mb total deformation	300-mb total deformation times wind speed
1000-500 mb mean relative humidity	950-500 mb vertical wind shear
700-mb v wind component	700-500 mb TI2 index

Table 4. Contingency table used in statistical analysis.

	Forecast		
Observed	CAT	No CAT	Total
CAT	x	y	x + y
No CAT	z	w	z + w
Total	x + z	y + w	x + y + z + w

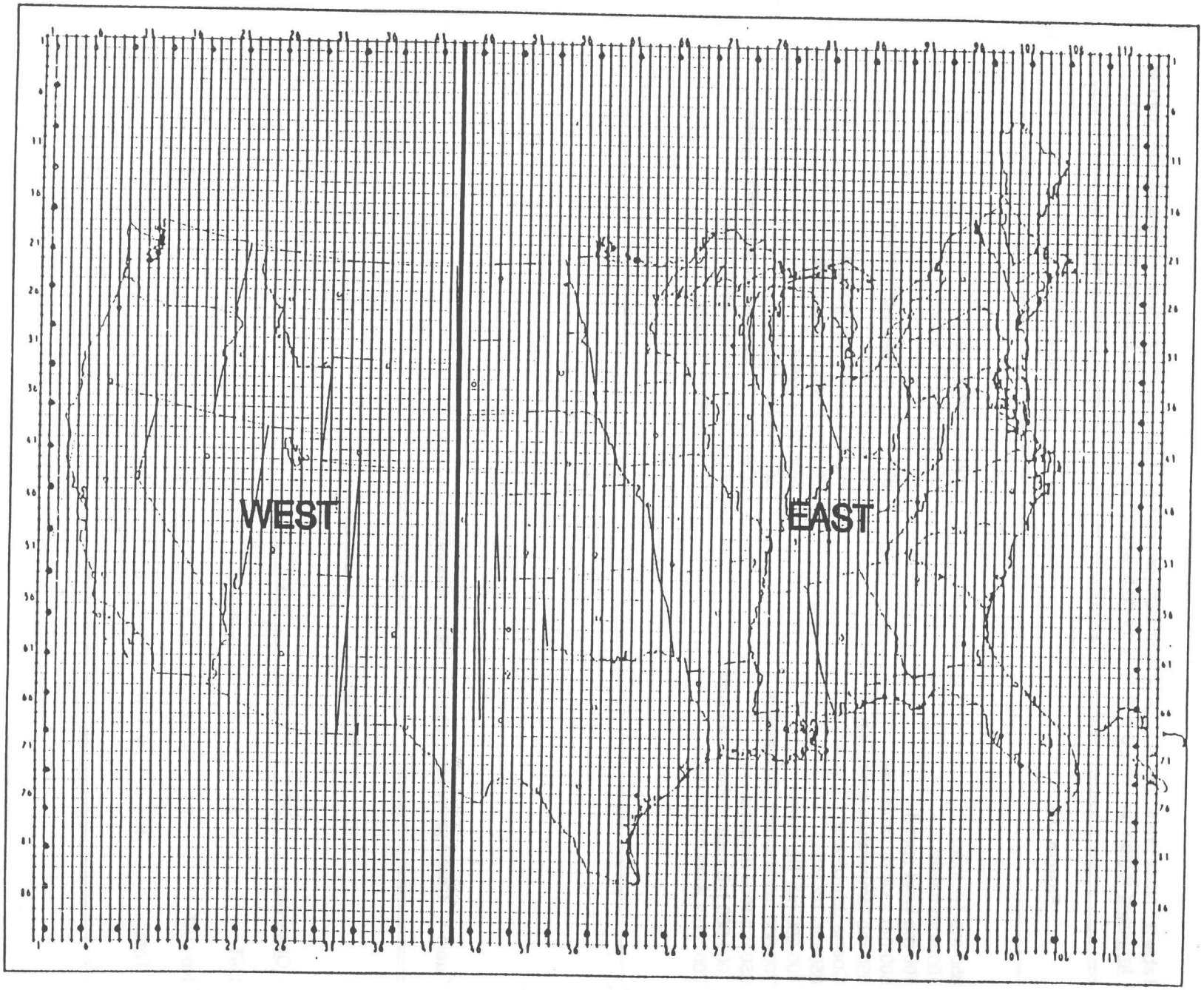

Figure 1. Development grid for MOS clear-air-turbulence probability equations. Mesh length for 89x113 grid is 48 km at 60 deg north.

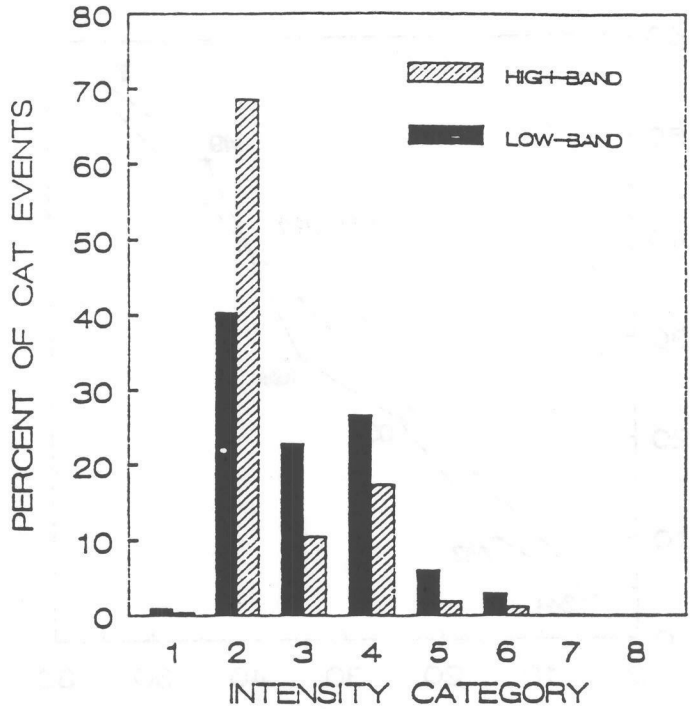

Figure 2. Distribution of high-band and low-band CAT reports for 1990 as a function of intensity category. Total number of reports was 62,639 (80,014) for the high-band (low-band) regions.

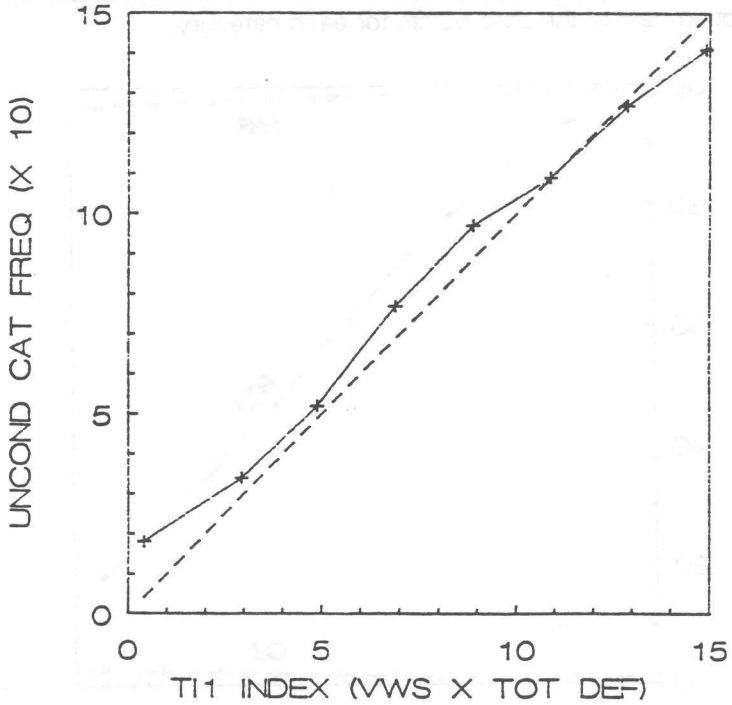

Figure 3. Unconditional frequency of category 3 or greater CAT in the eastern U.S. as a function of the TI1 index for the 20-26 h projection after 0000 UTC during the 1988-90 cool seasons.

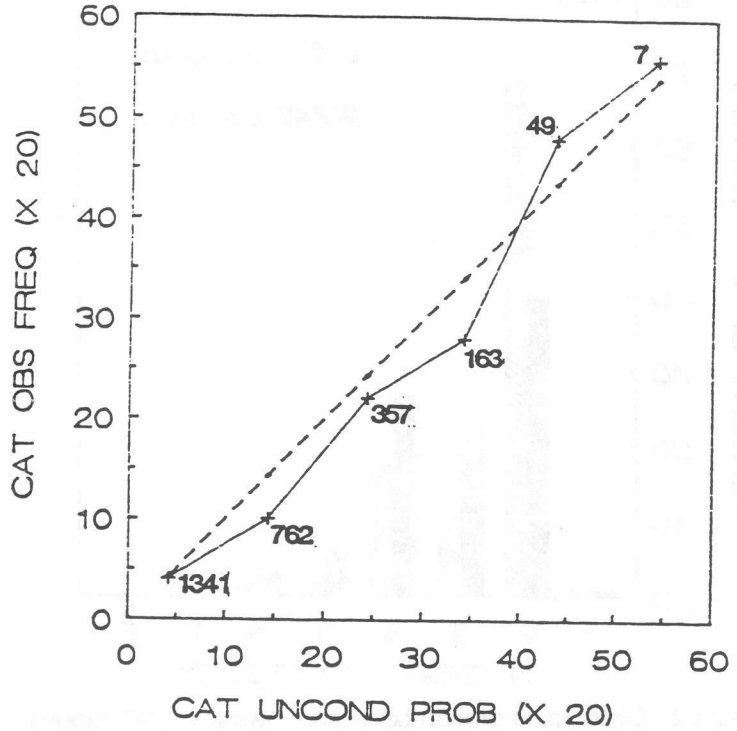

Figure 4. Reliability diagram for MOS CAT probability forecasts for 14-20 h projection after 0000 UTC. The scaled forecasts are valid for the high-band region for the October 1 - March 14 cool season period during 1988. Number of cases (hundreds) is plotted next to the data points for each category.

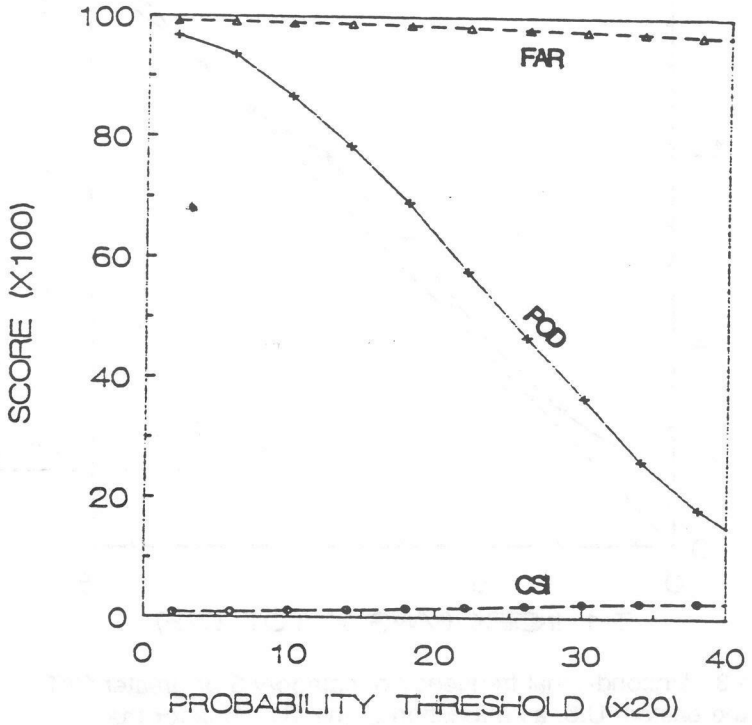

Figure 5. The critical success index (CSI), probability of detection (POD), and false alarm ratio (FAR) for categorical forecasts of category 3 or greater CAT based on various probability thresholds. Forecasts were for the high-band region for the 14-20 h projection after 0000 UTC during 1989-90 cool seasons.

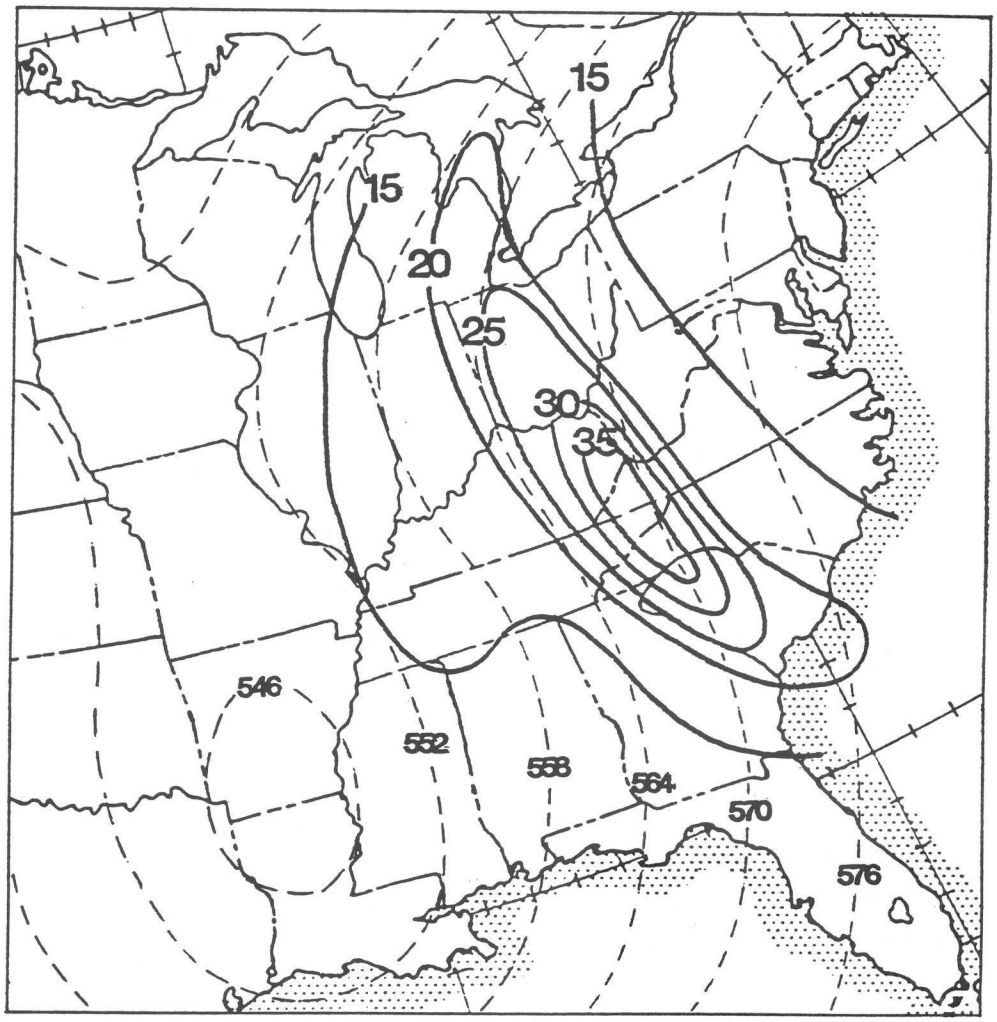

Figure 6. High-band scaled (x 20) probability contours (solid lines) for the occurrence of category 3 or greater CAT in 48-km grid blocks during the 8-14 h projection following 1200 UTC initial data time on Jan 14, 1995. 500-mb height contours for initial data time are shown by dashed lines.